*J. Electrochem. Sci. Eng.* ***16*** *(2026) 3619; https://doi.org/10.5599/jese.3619*

Open Access : : ISSN 1847-9286
https://pub.iapchem.org/ojs/index.php/JESE

*Original scientific paper*

# Synergistic modulation of electrochemical and structural properties in agarose: phytagel biopolymer blends as sustainable polymer electrolyte host matrices

Farisha Irdina Muhammad Ridzuan[1,2], Tan Winie[1,3], Annie Maria Mahat[1,3] and Siti Zafirah Zainal Abidin[1,2,✉]

[1]*Faculty of Applied Sciences, Universiti Teknologi MARA, 40450 Shah Alam, Selangor, Malaysia*
[2]*Ionic Materials and Devices (iMADE) Research Laboratory, Institute of Science, Universiti Teknologi MARA, 40450 Shah Alam, Selangor, Malaysia*
[3]*Center for Functional Materials and Nanotechnology, Institute of Science, Universiti Teknologi MARA, 40450 Shah Alam, Selangor, Malaysia*

*Corresponding Author:* ✉mailto:*szafirah@uitm.edu.my*

Received: July 1, 2026; Accepted: August 31, 2026; Published: September 5, 2026

***Abstract***

*The electrochemical stability and charge-transport properties of biopolymer blend films are significantly affected by blend composition, as each polymer component contributes uniquely to segmental mobility, bulk resistance, amorphous structure, and interfacial stability. In this study, salt-free agarose:phytagel (AG:PY) biopolymer blend films were fabricated at various weight ratios using the solution-casting method to identify an optimal host matrix for the development of salt-doped electrolytes. Linear voltammetry measurements showed that the 50:50 mass ratio AG:PY mixture has an electrochemical stability window of 3.25 V, indicating substantial resistance to electrochemical decomposition within the tested potential range. Electrochemical impedance spectroscopy analysis showed that the 50:50 blend achieved the highest room-temperature conductivity of 1.56 $\mu S\ cm^{-1}$, attributed to reduced bulk resistance and indicating more favourable charge-transport characteristics within the polymer host. X-ray diffraction analysis verified this finding, revealing the lowest crystallinity in the 50:50 mass ratio, suggesting increased amorphous content and greater polymer chain flexibility. Fourier-transform infrared spectroscopy spectral shifts confirmed interactions between the functional groups of agarose and phytagel, indicating improved blend compatibility. Collectively, the 50:50 mass ratio AG:PY blend exhibited the most advantageous combination of electrochemical stability, ionic conductivity, amorphous structure, and polymer interaction, establishing it as a promising sustainable host matrix for future salt-doped biopolymer electrolyte applications.*

**Keywords**
Polymer-polymer interaction; hydrogen bonding; solution casting; electrochemical stability; ionic conductivity; amorphicity

## Introduction

Rechargeable batteries are among the most extensively studied electrochemical energy-storage systems due to their ability to efficiently store and deliver electrical energy for use in portable electronics, electric vehicles, and renewable energy technologies [1]. Within these systems, the electrolyte is a critical component, providing the ion-conducting pathway between electrodes and significantly affecting ionic transport, electrode-electrolyte interfacial stability, safety, and overall electrochemical performance [2]. Conventional liquid electrolytes typically offer high ionic conductivity and effective electrode wettability [3]. Nevertheless, challenges such as leakage, flammability, volatility, and limited safety have prompted the development of solid and polymer-based electrolytes to enhance the safety of next-generation battery systems [4].

Polymer electrolytes have attracted considerable interest because they can serve as both an ion-conducting medium and a separator between electrodes, thereby simplifying cell design and enabling flexible, lightweight, and safer electrochemical devices [5]. Polymeric materials can also be tailored for mechanical strength, chemical resistance, dimensional stability, low weight, and ease of thin-film fabrication [6]. These benefits have driven extensive research into polymer electrolyte films for batteries, supercapacitors, fuel cells, sensors, and other flexible electrochemical systems [7-9]. However, polymer electrolytes based on single-polymer hosts often exhibit limited ionic conductivity at ambient temperature. This issue typically stems from the polymer matrix's rigidity and semi-crystalline structure, which restrict segmental motion and reduce charge-carrier mobility [10].

Several strategies have been investigated to enhance polymer electrolyte performance, such as copolymerization, grafting, plasticization, filler incorporation, and polymer blending [11]. Polymer blending is especially appealing because it is simple, cost-effective, and combines the advantages of multiple polymers without requiring new synthesis [4,11]. In polymer electrolyte systems, blending can modify crystallinity, increase amorphous content, improve chain flexibility, and introduce functional groups that facilitate ion coordination and transport. The success of a polymer blend depends largely on the compatibility and miscibility of its components, which influence structural organization, ion-conducting pathways, and overall electrochemical performance [12].

Recently, increasing attention has been directed toward sustainable biopolymers as environmentally friendly alternatives to conventional synthetic polymer hosts for energy storage applications [13]. However, many polymer-blend electrolyte systems still use synthetic, petroleum-based polymers, which are often non-biodegradable and pose disposal challenges [14]. Fully biopolymer-based blend systems remain less studied, even though they offer renewable, biodegradable, and functional host matrices for solid polymer electrolytes. Recent studies on biopolymer blend electrolytes, such as chitosan:methylcellulose [15], chitosan:dextran [16], and gellan gum:chitosan [17], demonstrate that biopolymer blending is a promising approach to enhance the host electrolyte's properties.

Agarose is a promising biopolymer for solid polymer electrolyte applications because of its renewable nature, biocompatibility, non-toxicity, film-forming ability, and abundant hydroxyl groups, which can coordinate with mobile ions upon salt incorporation [18]. However, the rigid, semicrystalline structure of agarose can restrict polymer chain mobility and limit ion transport [19]. The glass transition temperature ($T_g$) of dried pristine agarose film has been reported at

approximately 105.3 °C, reflecting its relatively rigid chain structure at room temperature [20]. Phytagel, a gellan-gum-based biopolymer, serves as a suitable blending partner due to its bio-compatibility, non-toxicity, thermal stability, and reactive hydroxyl and carboxyl groups, which facilitate intermolecular interactions and support polymer-salt coordination within the electrolyte matrix [21]. The reported $T_g$ of pure gellan gum is generally in the range of 40 to 60 °C [22,23]. However, some studies have indicated that its $T_g$ may be difficult to detect clearly by differential scanning calorimetry (DSC) due to crystallinity, moisture loss, or broad thermal transitions [24]. Compared with agarose, the lower reported $T_g$ of phytagel or gellan gum suggests that phytagel may contribute greater segmental mobility within the blend system. Consequently, blending agarose with phytagel is anticipated to disrupt agarose chain packing, reduce crystallinity, and increase the amorphous character of the polymer host. This interpretation aligns with findings from polymer blend electrolyte studies, where blending has been employed to reduce structural rigidity, enhance segmental mobility, and improve ion transport pathways [5,25]. Therefore, the AG:PY blend is proposed to provide a more favourable host matrix for future salt incorporation in solid polymer electrolyte systems.

Fully biopolymer-based agarose:phytagel (AG:PY) blend films were developed as potential host matrices for solid polymer blend electrolytes. The primary objective was to determine the optimal agarose-to-phytagel blend ratio prior to salt incorporation, as host-matrix optimization is critical for designing efficient polymer electrolytes for rechargeable battery applications. The blend films were fabricated using the solution casting method and characterized by linear sweep voltammetry (LSV), electrochemical impedance spectroscopy (EIS), X-ray diffraction (XRD), Fourier-transform infrared spectroscopy (FTIR) and field emission scanning electron microscopy (FESEM). LSV was employed to assess the electrochemical stability window of the salt-free blend films, while EIS was used to measure room-temperature bulk resistance and ionic conductivity. XRD was used to analyse changes in crystallinity and amorphous content, FTIR was used to identify functional group interactions and compatibility between agarose and phytagel, and FESEM was used to characterize the surface morphology of the biopolymer blend film. The observed correlations among electrochemical behaviour, ionic transport, structural disorder, and molecular interactions elucidate how (AG:PY) blending influences the formation of a sustainable biopolymer host matrix and identify the most suitable composition for subsequent salt incorporation and enhanced electrolyte performance.

## Experimental

### *Materials*

The agarose:phytagel biopolymer blend films were prepared using phytagel, a high-purity gelling polysaccharide obtained from the fermentation of *Sphingomonas elodea* and supplied by Sigma-Aldrich (USA). SeaKem® LE Agarose of molecular biology grade was obtained from Next Gene (Malaysia). Dimethyl sulfoxide (DMSO, ≥ 99.7 %) was purchased from Chemiz, Malaysia and used as the solvent for both polymers; all chemicals were used as received without prior treatment.

### *Synthesis of biopolymer blends*

AG:PY biopolymer blends were prepared by solution casting. A total of 0.5 g of polymer was mixed at mass ratios of 0:100, 10:90, 30:70, 40:60, 50:50, 60:40, 70:30, 90:10 and 100:0, then dissolved in 20 mL of DMSO and magnetically stirred for 2 weeks at room temperature to ensure homogeneity. The mass of each polymer, expressed in grams for each mass ratio, was calculated using Equation (1).

$$\text{Mass of polymer} = \left( \frac{\text{Polimer content}}{100} \right) 0.5 \quad (1)$$

where the polymer content is expressed as a percentage.

The solutions were cast into clean Petri dishes and dried in a vacuum oven at 70 °C to form uniform, colourless thin films. These films served as the final samples for characterization, as shown in Figure 1.

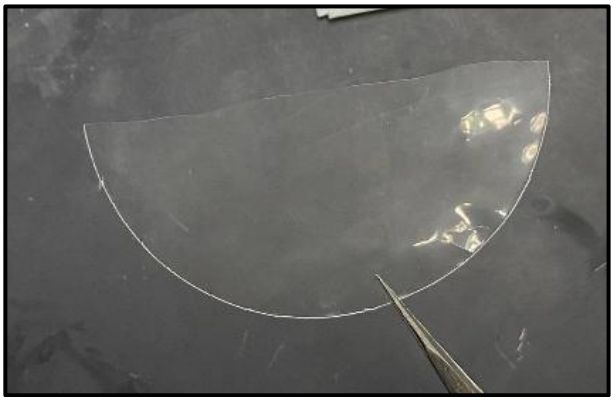

***Figure 1.*** *Thin film of agarose:phytagel biopolymer blend*

*Linear sweep voltammetry of biopolymer blend agarose:phytagel*

The electrochemical stability of the highest conducting sample will be evaluated using LSV with an Automatic Battery Cycler (WBCS 3000, WonA Tech, Seoul, South Korea). The sample will function as a separator, positioned between stainless steel (SS) and sodium (Na) metal electrodes. The measurement will be conducted at a scan rate of 5 mV $s^{-1}$, with the initial and final potentials set within the -5 to +5 V range. The current-voltage curve will be recorded to assess the electrochemical stability of the polymer electrolyte.

*Electrochemical impedance spectroscopy of biopolymer blend agarose:phytagel*

AG:PY biopolymer blends were cut into small pieces and sandwiched between two stainless steel plates. An HIOKI 3532-50 LCR Hi-tester at 300 K was used to measure impedance over the frequency range 100 Hz to 1 MHz. The ionic conductivity of the electrolytes was calculated using Equation (2):

$$\sigma = \frac{t}{R_b A} \quad (2)$$

where $\sigma$ is the DC conductivity, $t$ is the thickness of AG:PY biopolymer blend, $A$ is the contact surface area and $R_b$ is the bulk resistance. Bulk resistance was determined from the impedance plot, specifically at the intersection of the low-frequency semicircle and the rising spike on the real impedance axis. Using EIS analysis, samples were tested at room temperature (300 K) and placed in a humidity chamber to prevent external humidity effects. Samples were carefully positioned between the electrodes to ensure optimal contact at the electrode-electrolyte interface, resulting in more accurate EIS test outcomes.

*X-ray diffraction of biopolymer blend agarose:phytagel*

The structural appearance of the AG:PY biopolymer blends is crucial as supporting evidence that the system could exhibit improved amorphousness. Therefore, X-ray diffraction (XRD) spectra were analysed based on the constructive interference of monochromatic X-rays in a crystalline sample. The Bragg angle, $2\theta$ in the XRD diffractometer was varied from 5 to 90° at room temperature, and the

highest peak in the XRD spectra was interpreted as the degree of crystallinity of the AG:PY biopolymer blends using a PANalytical X'Pert PRO diffractometer with CuKα radiation ($\lambda$ = 0.1548 nm).

*Fourier transform infrared spectroscopy of biopolymer blend agarose:phytagel*

Molecular interactions in electrolyte systems were identified using FTIR spectroscopy. The spectrum showed interactions between biopolymer agarose and phytagel in the blending system. Spectral measurements were based on infrared absorption, which identified specific features of the electrolytes' components and structures. In this study, FTIR spectra were recorded using a PerkinElmer Model 400 spectrometer over the spectral range 650 to 4000 $cm^{-1}$ with a resolution of 4 $cm^{-1}$.

*Field emission scanning electron microscopy of biopolymer blend agarose:phytagel*

The surface morphology of the biopolymer blend agarose:phytagel was examined using a Thermo Fisher Apreo 2 Scanning Electron Microscope, achieving a magnification of up to 50,000×. The FESEM technique will be employed to examine the morphological characteristics and surface uniformity of the samples, providing insights into component dispersion and the overall structural integrity of the polymer electrolyte films.

## Results and discussion

*Linear sweep voltammetry analysis*

The electrochemical stability of salt-free AG:PY polymer blend films was assessed using linear sweep voltammetry (LSV). Measurements were performed at room temperature using an SS//polymer blend film//Na metal configuration, over a potential range of -5 to +5 V at a constant scan rate of 5 mV $s^{-1}$. This scan rate was consistently applied to all compositions to enable direct comparison of their current-voltage responses and estimated electrochemical stability windows.

The current response observed in an LSV curve characterizes the electrochemical behaviour of the polymer film during an applied potential sweep. A low and nearly constant current suggests that the film remains stable, with no significant Faradaic reactions or electrochemical degradation occurring within that potential range [26]. In this study, the positive onset voltage corresponds to oxidative decomposition ($V_{ox}$), while the negative onset voltage corresponds to reductive decomposition ($V_{red}$). The electrochemical stability window ($\Delta V$) was determined using Equation (3).

$$\Delta V = V_{ox} - V_{red} \quad (3)$$

Because the current AG:PY films were salt-free, the observed LSV response is not primarily related to salt-ion redox activity. The increase in current at high applied potentials is instead attributed to electrochemical degradation of the polymer host matrix or to interfacial reactions at the electrode and polymer-film interfaces. Consequently, the LSV parameters obtained in this study serve as comparative indicators of the electrochemical tolerance of salt-free polymer host films prior to salt incorporation.

The anodic and cathodic current responses were evaluated at terminal potentials of +5 and -5 V, respectively. The anodic current corresponds to the positive potential region and is associated with oxidative reactions or oxidative degradation of the polymer film at elevated applied voltages [27]. In contrast, the cathodic current corresponds to the negative potential region and is linked to reductive reactions or cathodic interfacial processes [28]. An increase in current during the potential sweep typically indicates electrochemical instability, whereas a reduced current response suggests enhanced electrochemical stability [29].

Figure 2(a) presents the LSV curves for pristine agarose and phytagel. The pristine agarose (100:0 mass ratio) film exhibits a stronger anodic current response at high positive voltages, indicating more pronounced oxidative activity beyond the onset region [30]. In contrast, the pristine phytagel (0:100 mass ratio) film displays a stronger cathodic current response at more negative voltages, reflecting a more pronounced reduction-side current. Figure 2(b) displays the LSV curves for blended AG:PY films. The AG:PY blend films show a low-current region across the intermediate potential range, suggesting the polymer films remain stable before decomposition. At elevated positive potentials, a marked increase in anodic current is observed, which is attributed to oxidative decomposition of the polymer host film. The increase in cathodic current at negative potentials indicates reductive decomposition or interfacial reactions. Variations in onset voltage, terminal current response, and stability window among the blend ratios indicate that the electrochemical stability of the films is composition-dependent.

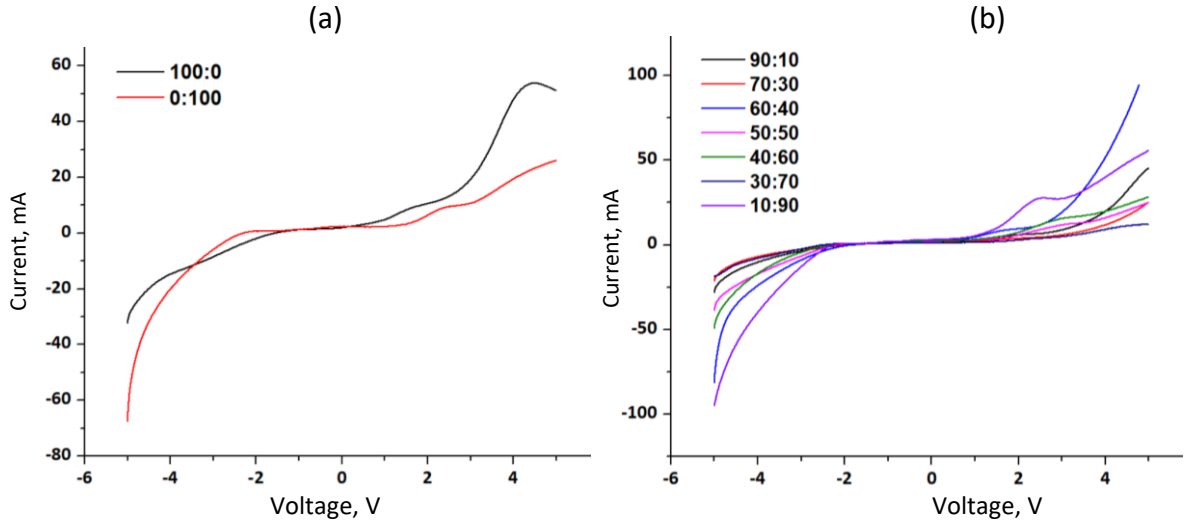


***Figure 2.*** *LSV curves of (a) pristine agarose and pristine phytagel films and (b) agarose:phytagel blend films at different composition ratios*

The LSV parameters in Table 1 indicate that the 30:70 mass-ratio blend has the widest electrochemical stability window (3.49 V), reflecting the greatest potential tolerance under fixed LSV conditions. This blend also exhibits a relatively low terminal current response, indicating reduced electrochemical activity at the voltage limits. In contrast, the 50:50 mass ratio blend achieves the highest oxidative decomposition onset voltage ($V_{ox}$) of 1.38 V and retains a relatively broad stability window of 3.25 V. Similar composition-dependent electrochemical behaviour has been observed in PEO/PVDF blend films, where adding PVDF increases current response compared to pure PEO, indicating improved charge transport in the blend [31]. These results suggest that the 50:50 mass ratio offers superior resistance to oxidative decomposition, despite a slightly narrower overall stability window than the 30:70 blend.

LSV analysis indicates that both 30:70 and 50:50 mass ratios exhibit favourable electrochemical stability. The 30:70 mass ratio blend offers the broadest electrochemical stability window, while the 50:50 mass ratio blend displays the greatest resistance to oxidative decomposition. However, electrochemical stability alone does not determine the optimal polymer host matrix. Therefore, the LSV results were correlated with analyses of ionic conductivity, crystallinity, and molecular interactions. This comprehensive evaluation is necessary because an ideal polymer electrolyte host should combine a sufficiently wide electrochemical stability window with efficient ion-transport pathways, low crystallinity, and strong polymer-polymer interactions. Although the 30:70 mass ratio

blend provides the widest stability window, the 50:50 mass ratio remains a promising host matrix when its oxidative stability is considered alongside the EIS, XRD, and FTIR results.

***Table 1.*** *LSV parameters of salt-free agarose:phytagel blend films*

| AG:PY mass ratio | Cathodic current at -5 V, mA | Anodic current at +5 V, mA | $V_{red}$ / V | $V_{ox}$ / V | $\Delta V$ / V |
|---|---|---|---|---|---|
| 100:0 | -32.14 | 51.07 | -1.46 | 0.43 | 1.89 |
| 90:10 | -28.16 | 45.40 | -2.13 | 0.53 | 2.66 |
| 70:30 | -21.31 | 25.17 | -2.05 | 0.73 | 2.78 |
| 60:40 | -81.26 | 94.29 | -2.28 | 0.59 | 2.87 |
| 50:50 | -38.75 | 24.83 | -1.87 | 1.38 | 3.25 |
| 40:60 | -49.29 | 28.27 | -1.95 | 1.12 | 3.07 |
| 30:70 | -18.88 | 12.15 | -2.16 | 1.33 | 3.49 |
| 10:90 | -94.89 | 55.64 | -2.23 | 0.91 | 3.14 |
| 0:100 | -67.36 | 25.96 | -2.19 | 1.15 | 3.34 |

*Electrochemical impedance spectroscopy analysis*

In electrochemical energy-storage systems, the polymer host matrix provides a continuous medium for ion migration after salt incorporation. Evaluating the impedance response of salt-free polymer blends is an essential preliminary step to understand how polymer composition affects intrinsic bulk resistance, charge-transport pathways, and electrode-film interfacial behaviour [32-34]. Although no external salt was added in this study, EIS still offers valuable insights into the inherent electrical response of AG:PY blend films. This response may result from polar functional groups, residual mobile species, absorbed moisture, and dielectric polarization within the biopolymer network.

Figure 3 illustrates the potential intermolecular interactions between agarose and phytagel. The schematic depicts possible hydrogen-bond formation between the hydroxyl groups of agarose and the hydroxyl or carboxyl groups of phytagel. Such interactions suggest strong compatibility between the two biopolymer matrices. Intermolecular hydrogen bonding may disrupt the regular packing of polymer chains, leading to a less ordered structure with enhanced segmental mobility. Furthermore, the presence of polar groups, especially hydroxyl and carboxyl groups from phytagel, can provide intrinsic sites for localized charge transport and hopping processes. Thus, the interaction depicted in Figure 3 supports the role of AG:PY blending in enhancing the electrical response of salt-free polymer films.

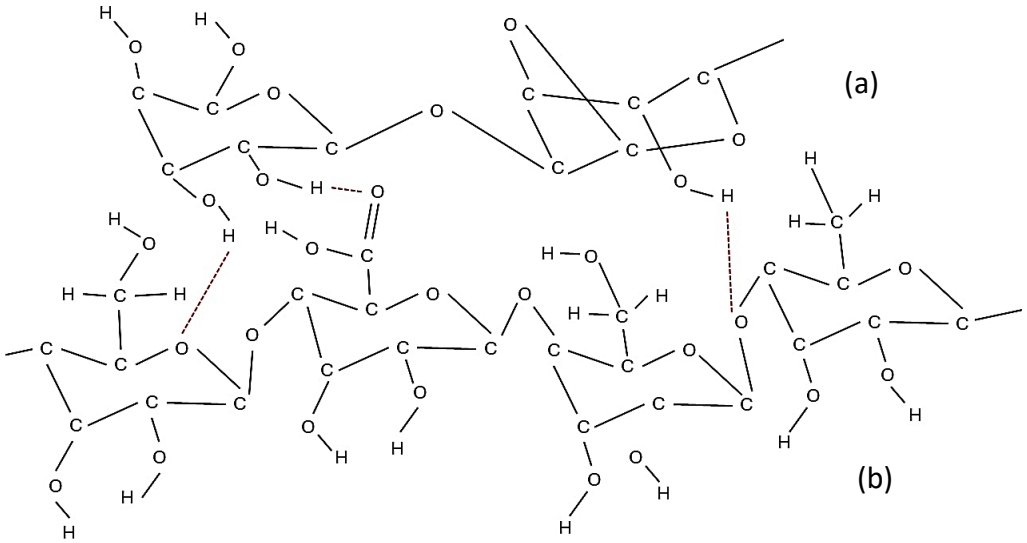


***Figure 3.*** *Schematic diagram of possible interactions between (a) agarose and (b) phytagel structure (where ------ represents interactions within polymers)*

EIS was used to evaluate the ionic conductivity of the AG:PY biopolymer blend films. As shown in Figure 4 and tabulated in Table 2, the ionic conductivity increased from 4.20 nS $cm^{-1}$ for the pristine agarose film to a maximum value of 1.56 μS $cm^{-1}$ at the 50:50 AG:PY mass ratio. The enhanced conductivity observed in the 50:50 mass ratio blend suggests that this composition offers the most favourable polymer-host environment for charge transport. This improvement is attributed to a more flexible and less ordered polymer matrix, which promotes segmental motion and facilitates ion hopping within the blend film. As demonstrated by the XRD analysis, the 50:50 mass ratio exhibits the lowest crystallinity, indicating a higher amorphous fraction in the polymer matrix. The increased amorphous region enhances charge migration by providing greater chain flexibility and more accessible transport pathways [35]. Consequently, the superior conductivity of the 50:50 mass ratio blend likely results from a synergistic interaction between agarose and phytagel that disrupts the ordered polymer arrangement and yields a more amorphous structure suitable for electrolyte applications. Combined with the LSV response, which demonstrates electrochemical stability within the applied potential range, the EIS result indicates that the 50:50 mass ratio blend facilitates charge transport and preserves electrochemical stability as a salt-free host matrix.

However, increasing phytagel content beyond a certain point did not further improve conductivity. The reduced conductivity in phytagel-rich compositions may result from greater structural rigidity, stronger intermolecular interactions, or reduced chain mobility [36,37]. While phytagel's polar and carboxylate groups can enhance charge response, excessive phytagel can create a rigid or brittle film that limits charge migration [38]. Therefore, the 50:50 AG:PY mass ratio blend is identified as the optimum composition for further salt incorporation.

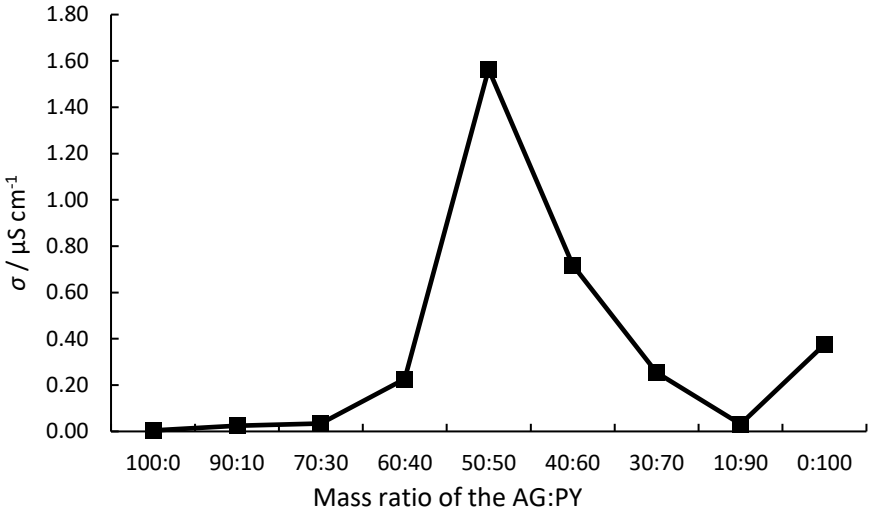


***Figure 4.*** *Room-temperature ionic conductivity of biopolymer blend, AG:PY systems*

***Table 2.*** *Bulk resistance and ionic conductivity at room temperature for the biopolymer blend AG:PY systems*

| AG:PY mass ratio | $t$ / μm | $A$ / $cm^2$ | $R_b$ / MΩ | $\sigma$ / μS $cm^{-1}$ |
|---|---|---|---|---|
| 100:0 | 60 | 0.2818 | 5.30 | 0.00420 |
| 90:10 | 50 | 0.2818 | 0.722 | 0.0249 |
| 70:30 | 50 | 0.2818 | 0.524 | 0.0339 |
| 60:40 | 30 | 0.2818 | 0.047 | 0.227 |
| 50:50 | 60 | 0.2818 | 0.0136 | 1.56 |
| 40:60 | 30 | 0.2818 | 0.0151 | 0.718 |
| 30:70 | 70 | 0.2818 | 0.122 | 0.253 |
| 10:90 | 60 | 0.2818 | 0.684 | 0.0312 |
| 0:100 | 70 | 0.2818 | 0.0665 | 0.376 |

*X-ray diffraction analysis*

Figure 5 displays the XRD patterns of agarose and phytagel powders. Phytagel (Figure 5b) exhibits two distinct, high-intensity peaks, consistent with previous findings [39]. The narrow and intense nature of these peaks suggests the semicrystalline structure of the host polymer, phytagel [21]. In contrast, the diffraction pattern for pure agarose, also shown in Figure 5a, displays a broad hump around 19.05°, a feature associated with the semi-amorphous nature of agarose films [40].

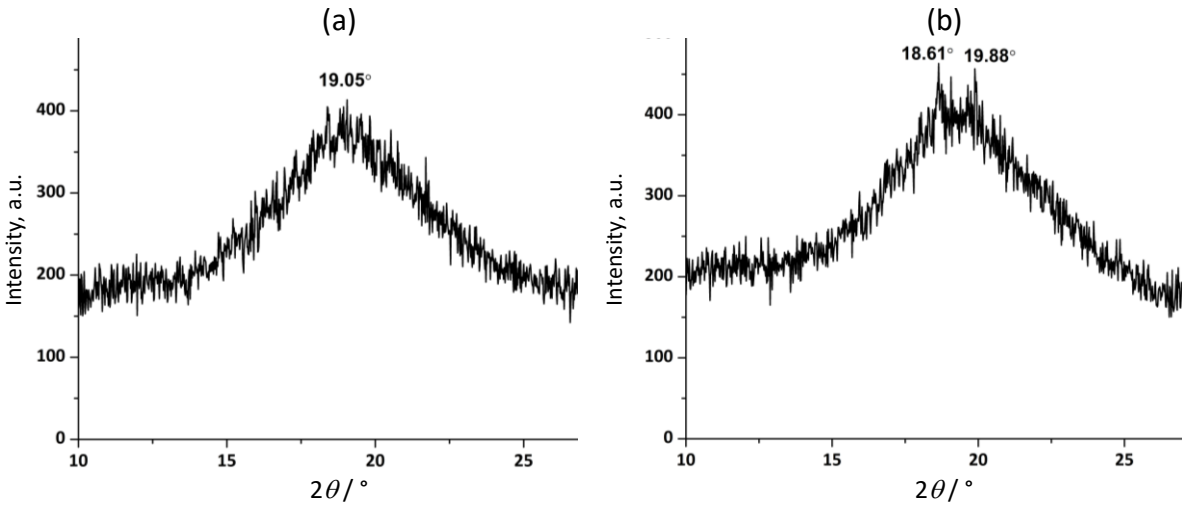


***Figure 5**. XRD pattern of (a) 0.5 g agarose and (b) 0.5 g phytagel powder*

Figure 6 displays the XRD patterns of AG:PY polymer blend films at various composition ratios. Figures 6(b) to (h) indicate that increasing agarose content in phytagel reduces the intensity of the semicrystalline peaks associated with phytagel.

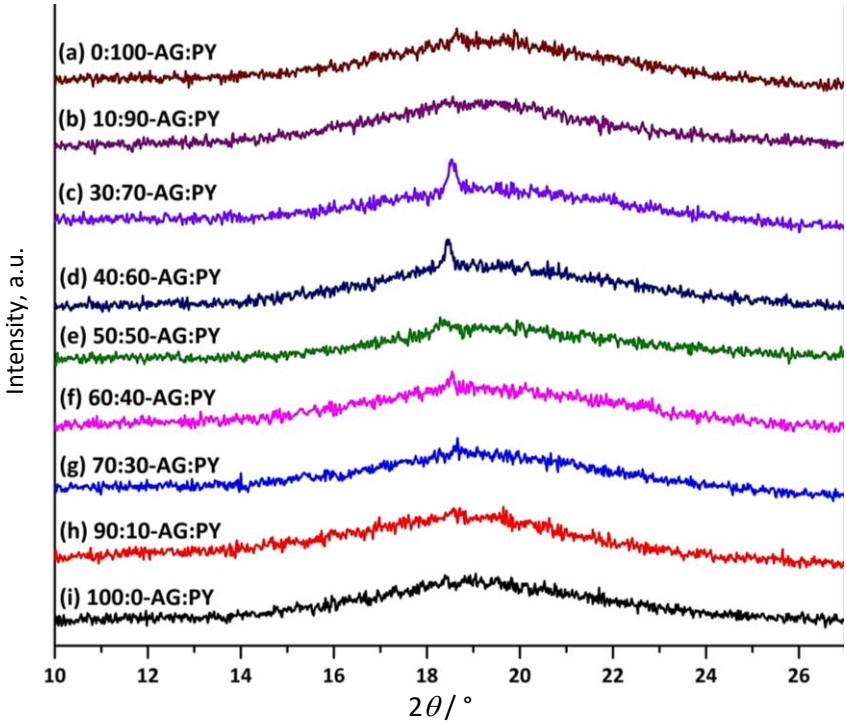


***Figure 6**. XRD stacking graph pattern of biopolymer blend AG:PY, with different ratios*

This reduction implies an increase in the amorphous phase, likely due to the disruption of the ordered arrangement of phytagel chains [41]. The amorphous phase lowers the energy barrier for the movement of polymer chain segments. As a result, conductivity goes up when the sample has a

larger amorphous region [11,42]. The sample with the largest amorphous domain is expected to exhibit the highest electrical conductivity at room temperature. To demonstrate this effect, electrical conductivity measurements were conducted on the samples.

The results indicate that AG:PY polymer blend films exhibit both crystalline and amorphous phases. Crystallinity in all samples was measured, and crystalline peaks were identified using a combination of scattered intensities. The degree of crystallinity ($X_c$ / %) was determined by comparing the area under the crystalline peak to the area under the amorphous halos. To separate these peaks, the XRD patterns for all polymer blend compositions were deconvoluted using Equation (4)

$$X_C = \frac{A_c}{A_c + A_a} 100 \quad (4)$$

where $A_c$ and $A_a$ represent the areas of the crystalline peak and amorphous halo, respectively.

Table 3 presents the peak centre and full width at half maximum (FWHM) values obtained from Gaussian deconvolution of the XRD patterns. Figure 7 displays the corresponding fitted profiles for the AG:PY blend films. The diffraction patterns were resolved into three or four Gaussian components due to the overlapping crystalline and amorphous contributions of the two polymers. The degree of crystallinity was calculated from the deconvoluted peak areas and is reported in Table 3. The $X_c$ values decreased from 61.484 % for pure agarose to a minimum of 31.994 % at the 50:50 AG:PY mass ratio, then increased for phytagel-rich films. These results indicate that the 50:50 blend mass ratio exhibits the lowest crystalline fraction and the highest amorphous character among all compositions.

***Table 3.*** *Centre, full-width at half maximum of the deconvoluted XRD peaks and the degree of crystallinity for AG:PY biopolymer blend films with varying compositions*

| AG:PY mass ratio | First peak | | Second peak | | Third peak | | Fourth peak | | $X_c$ / % |
|---|---|---|---|---|---|---|---|---|---|
| | Centre | FWHM | Centre | FWHM | Centre | FWHM | Centre | FWHM | |
| 100:0 | 18.757 | 5.123 | 21.167 | 9.492 | - | - | - | - | 61.484 |
| 90:10 | 18.825 | 4.899 | 21.210 | 8.795 | 13.654 | 3.660 | - | - | 57.117 |
| 70:30 | 18.143 | 4.887 | 11.786 | 1.836 | 20.225 | 6.057 | - | - | 41.978 |
| 60:40 | 20.197 | 4.996 | 26.299 | 1.691 | 18.325 | 4.169 | - | - | 34.923 |
| 50:50 | 19.349 | 4.826 | 21.658 | 7.663 | 18.503 | 6.575 | - | - | 31.994 |
| 40:60 | 18.440 | 3.222 | 15.886 | 2.698 | 20.706 | 4.705 | - | - | 47.066 |
| 30:70 | 18.684 | 0.483 | 19.899 | 2.799 | 17.523 | 2.955 | 21.376 | 5.202 | 54.366 |
| 10:90 | 19.139 | 4.045 | 16.196 | 2.767 | 20.874 | 9.033 | - | - | 55.556 |
| 0:100 | 18.328 | 4.552 | 20.961 | 5.142 | - | - | - | - | 50.069 |

Figure 8 shows the variation in the degree of crystallinity of AG:PY biopolymer blend films at different composition ratios. Crystallinity decreases as the phytagel content increases from 100:0 to 50:50 mass ratio, then increases again in phytagel-rich blends. XRD deconvolution demonstrates that the 50:50 mass ratio blend exhibits the lowest crystallinity, indicating the most effective disruption of polymer chain ordering and the highest amorphous character. Therefore, this composition is considered the most suitable polymer host matrix for polymer electrolyte applications. Due to the considerable overlap between the diffraction peaks of agarose and phytagel, the precise number and assignment of the fitted peaks remain uncertain. Consequently, the crystallinity values should be interpreted in conjunction with the electrochemical findings from LSV and EIS, as well as the functional-group interactions supported by FTIR analysis.

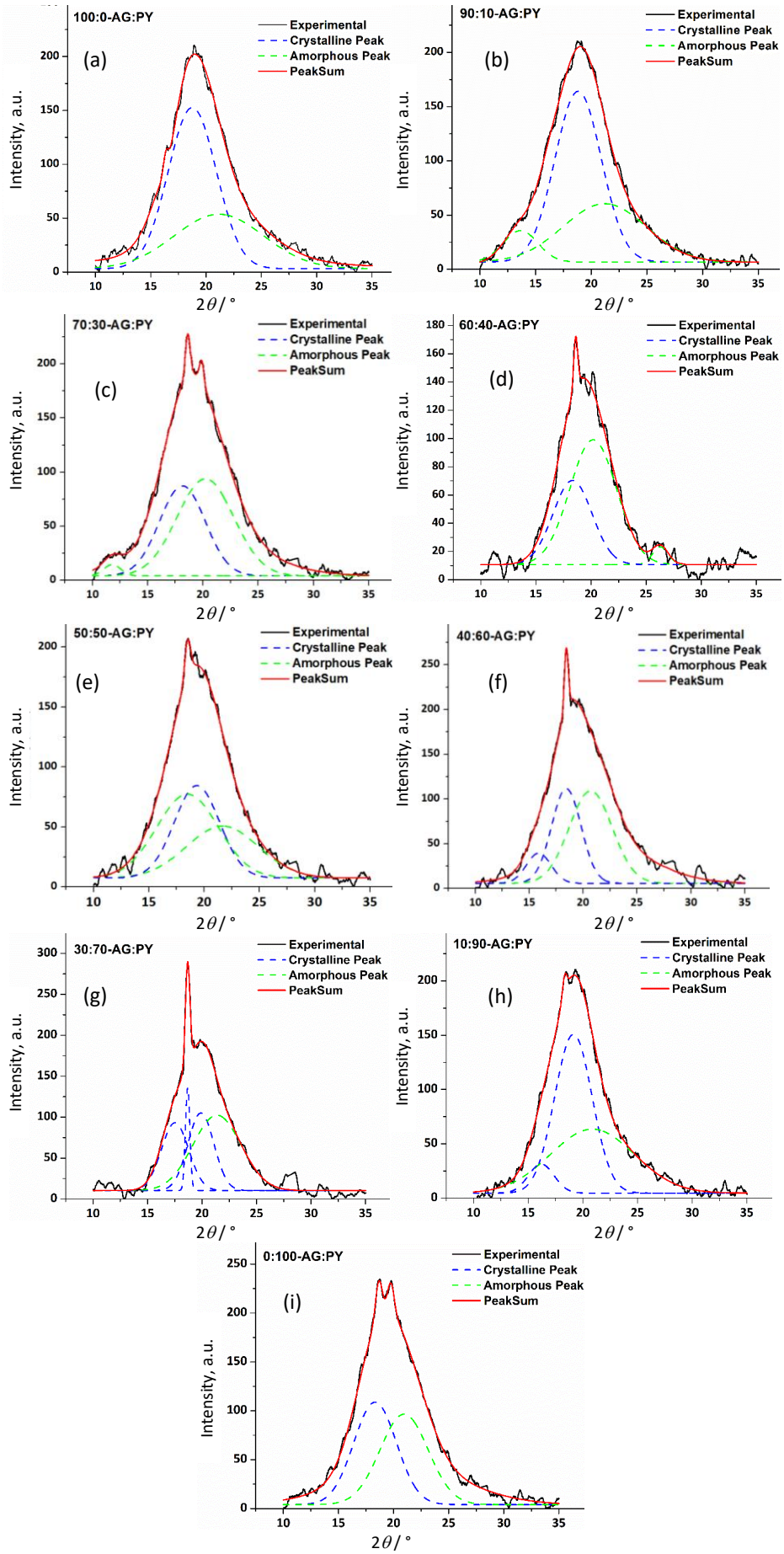


***Figure 7.*** *Deconvoluted XRD patterns of AG:PY biopolymer blend films with mass ratio of (a) 100:0, (b) 90:10, (c) 70:30, (d) 60:40, (e) 50:50, (f) 40:60, (g) 30:70, (h) 10:90 and (i) 0:100*

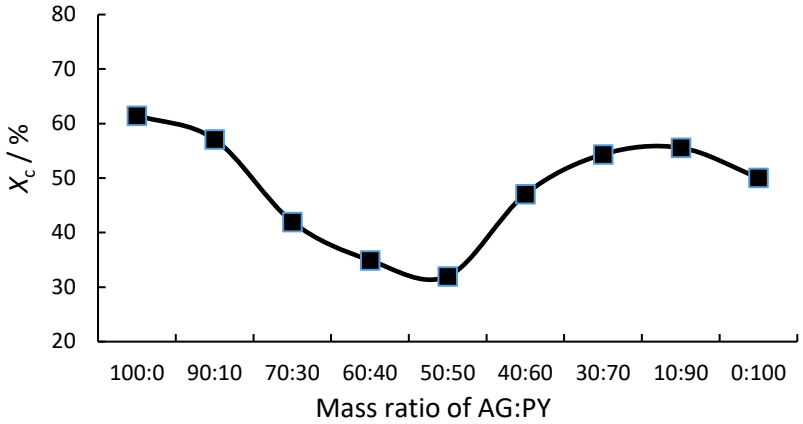


***Figure 8.*** *Degree of crystallinity of AG:PY biopolymer blend films at different mass ratios*

*Field emission scanning electron microscopy analysis*

Figure 9(a) shows the FESEM image of pristine agarose, which has irregular plate-like regions. There are noticeable agglomerates and scattered smaller fragments, pointing to a heterogeneous structure. Large, separated domains suggest that the agarose matrix is not packed uniformly. This irregular shape might increase the surface area, but agglomeration can lower the effective surface area, as seen in previous studies [43]. These compact areas may limit polymer-chain mobility and create less continuous paths for charge transport.

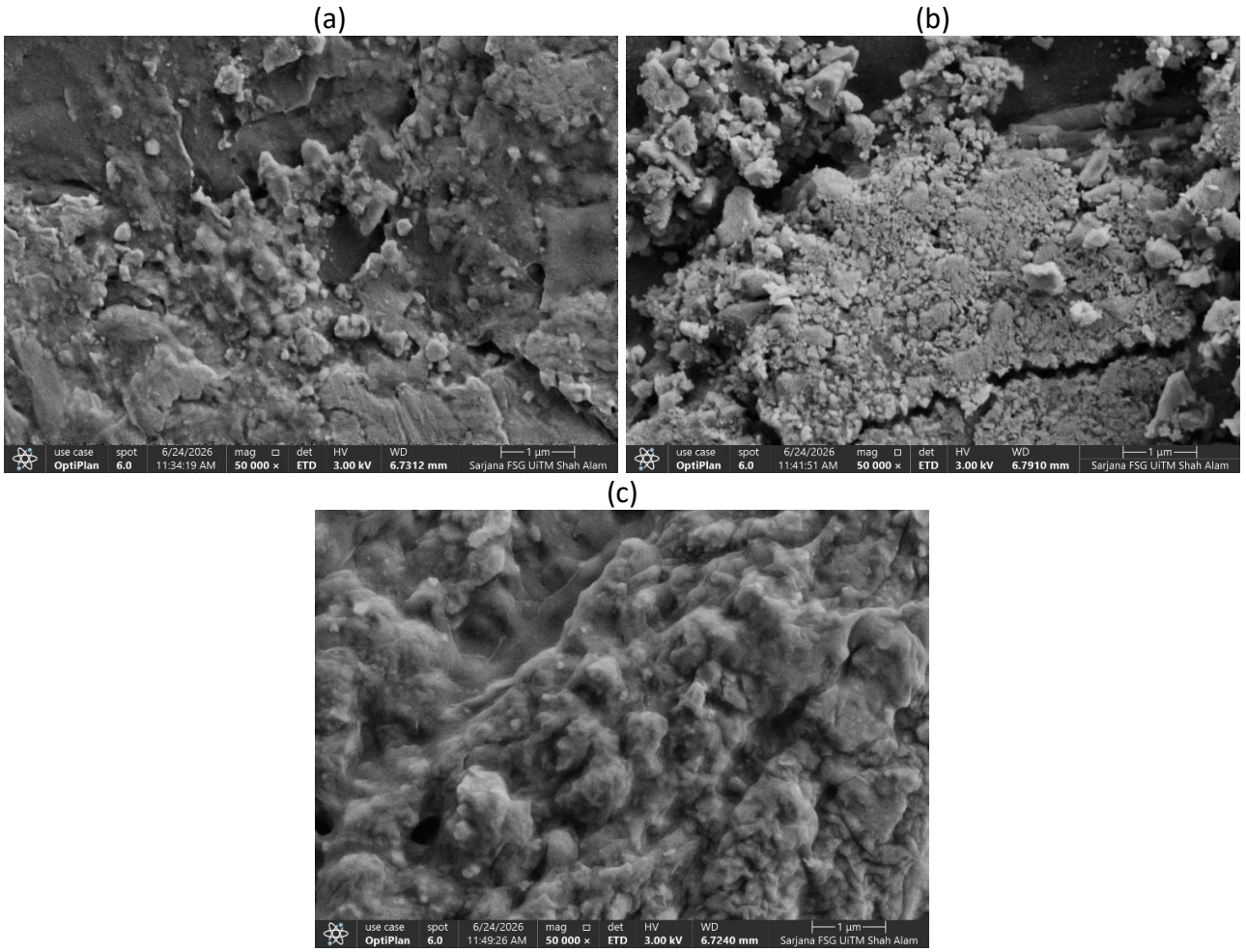


***Figure 9.*** *The FESEM images for (a) pristine agarose, (b) pristine phytagel and (c) 50:50 mass ratio of polymer blend agarose:phytagel*

Figure 9(b) presents the FESEM image of pristine phytagel, revealing a rough and granular surface morphology with numerous fine particles and agglomerated clusters. The relatively large voids between these clusters indicate a less compact and less cohesive structure, which may contribute to the brittle nature of pristine phytagel films. In addition, the heterogeneous distribution of clustered regions and voids may disrupt the continuity of transport pathways within the polymer matrix, potentially limiting efficient charge transport.

Figure 9(c) is the FESEM image of the ratio that produces the highest value of conductivity and the lowest value of crystallinity, which is the 50:50 mass ratio. Compared with both pristine polymers, the 50:50 mass-ratio blend shows a more interconnected and cohesive morphology. The individual plate-like agarose structures and strongly granular phytagel agglomerates are less distinguishable, suggesting that the two polymers are incorporated into a common blended matrix. The surface remains rough and contains some pores, but the polymer domains appear more closely connected and better distributed. The reduced appearance of separate agarose-rich and phytagel-rich regions may indicate improved compatibility between the two polymers.

*Fourier transform infrared spectroscopy analysis*

FT-IR spectroscopy was used to investigate the chemical composition and potential interactions in AG:PY biopolymer blend films. Complex formation between the two polymers arises from specific interactions within and between the polymer chains. Changes in the position, shape, and strength of the infrared absorption bands help identify interactions between the materials. Figure 10 presents the recorded FTIR spectra of all samples over the wavenumber range of 650 to 4000 $cm^{-1}$. The corresponding data are also provided in Table 4.

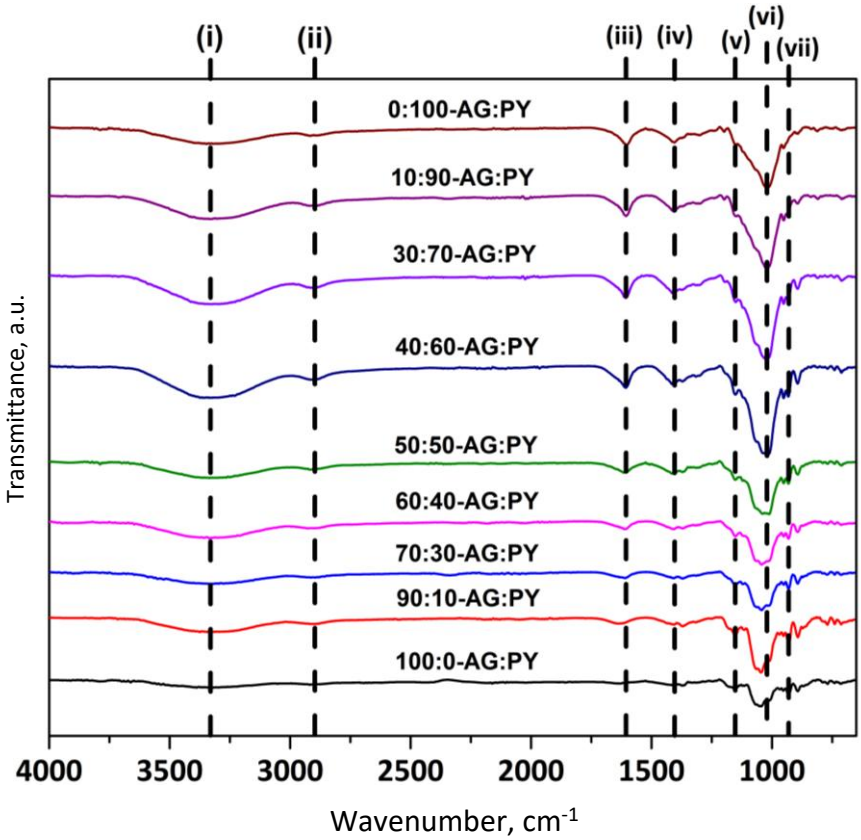


***Figure 10.*** *FT-IR spectra illustrating the composition of agarose and phytagel as polymer hosts within the polymer blend system*

The FT-IR spectra of AG:PY blend films exhibit characteristic absorption bands associated with polysaccharides, as shown in Figure 10 and tabulated in Table 4. Figure 10 illustrates that band (i) appears as a broad absorption band at 3316 $cm^{-1}$ across all compositions, corresponding to O–H stretching vibrations. The broadness of this band indicates intermolecular hydrogen-bonding interactions, and its consistent presence suggests that the immediate polysaccharide structure is preserved following blending. Band (ii), observed near 2908 $cm^{-1}$, is attributed to aliphatic C–H stretching and becomes less intense in agarose-rich films. This reduction is more plausibly related to compositional changes and potential band overlap rather than direct alterations in bond length [44]. Bands (iii) and (iv) exhibit increased intensity with higher phytagel content, indicating a greater contribution from the glucuronic acid-containing phytagel phase. These bands are more precisely attributed to carbonyl or carboxylate-related vibrations, with band (iii) corresponding to C=O stretching of keto-aldehyde or carboxyl groups in phytagel. In contrast, bands (v) and (vi) correspond to C–O–C and C–O stretching vibrations of the polysaccharide backbone and are observed in all blend compositions, confirming that the primary backbone structure is preserved after blending. Band (vii) is more pronounced in agarose-rich films and corresponds to the characteristic agarose region at approximately 890 to 930 $cm^{-1}$ [45,46].

***Table 4.*** *Significant FTIR absorption peaks of AG:PY biopolymer blend systems*

| No. | Wavenumber, $cm^{-1}$ | | | Assignment bands | References |
|---|---|---|---|---|---|
| | Agarose | Phytagel | Experimental | | |
| i | 3311 | 3320 | 3316 | O-H stretching (hydroxyl group) | [47,48] |
| ii | 2918 | 2919 | 2908 | Aliphatic C–H stretching | [22,47] |
| iii | - | 1605 | 1611 | C=O stretching | [48] |
| iv | - | 1404 | 1404 | C-C local symmetric stretching | [48] |
| v | 1154 | 1040 | 1151 | C-O-C stretching | [39,40] |
| vi | 1067 | 1026 | 1026 | C–O stretching | [48,40] |
| vii | 932 | - | 897 | 3,6-anhydrogalactose | [40] |

FT-IR analysis of the 50:50 blend ratio film shows the coexistence of characteristic functional groups from both agarose and phytagel, with slight shifts and broadening in the O–H and C–O/C–O–C regions. The observed broadening and shifting of the O–H band indicate the presence of intermolecular hydrogen bonding between agarose and phytagel. Additionally, the detection of ether and carboxylate-related groups suggests the availability of polar sites within the polymer matrix. These functional-group interactions are significant for electrochemical performance, as they disrupt the original chain packing of the individual polymers, enhance the amorphous character, and improve polymer-chain segmental mobility. This interpretation aligns with the EIS results, which show that the 50:50 mass ratio blend film exhibits lower bulk resistance and the highest ionic conductivity. The chemically interactive and less ordered polymer matrix thus provides a more favourable pathway for charge transport.

## Conclusion

A sustainable agarose:phytagel (AG:PY) biopolymer host was successfully prepared using the solution casting method for potential application in salt-doped biopolymer electrolyte films. LSV analysis showed that the 50:50 AG:PY mass ratio blend exhibited an electrochemical stability window of 3.25 V, indicating adequate stability within the applied potential range. Although the 30:70 mass ratio blend demonstrated a wider stability window, the 50:50 mass ratio exhibited superior overall performance when considering its possible electrical and structural properties. EIS

measurements at room temperature revealed that the 50:50 mass ratio blend achieved the highest conductivity of 1.56 μS $cm^{-1}$, indicating more favourable charge-transport characteristics within the polymer host. Structural analysis further demonstrated that this composition exhibited reduced crystallinity and a higher amorphous fraction, which correlated with its enhanced electrical conductivity. FTIR spectroscopy confirmed intermolecular interactions between agarose and phytagel, particularly through the shifting and broadening of the O–H stretching band, suggesting hydrogen-bond formation and good compatibility between the two biopolymers. Overall, the 50:50 AG:PY mass ratio provided the most favourable balance of electrochemical stability, conductivity, amorphous character, and intermolecular interactions, supporting its selection as the optimal host matrix for subsequent salt incorporation in biopolymer electrolyte systems.

***Acknowledgments:*** *The authors acknowledge the Ministry of Higher Education (MOHE) Malaysia for funding this research under the Fundamental Research Grant Scheme (FRGS) (referral code: FRGS/1/2025/STG05/UITM/02/1). The authors would like to thank the iMADE Research Laboratory, Institute of Science, and Faculty of Applied Sciences, Universiti Teknologi MARA (UiTM) for providing research facilities to carry out this project.*

***Funding:*** *This research was funded by the Ministry of Higher Education (MOHE) Malaysia under the Fundamental Research Grant Scheme (FRGS) (referral code: FRGS/1/2025/STG05/UITM/02/1).*

***Authors' declaration:*** *Farisha Irdina Muhammad Ridzuan: writing original draft, investigation and data curation; Siti Zafirah Zainal Abidin: writing, review & editing, supervision, project administration and funding acquisition; Tan Winie: supervision and conceptualization; Annie Maria Mahat: supervision and conceptualization.*

***Data availability:*** *The data and code that support the findings of this study are available from the corresponding author upon reasonable request.*

***Declaration of Generative AI and AI-assisted technologies in the writing process:*** *During the preparation of this work, the author(s) used AI-assisted technologies to refine language and improve readability.*

***Declaration of competing interests:*** *The authors declare that they have no known competing financial interests or personal relationships that could have appeared to influence the work reported in this paper.*

## References

[1] A. Makeyaw, T. Dame, M. Getu, D. Goytom, M. Tadese, T. Malto, Y. Gebremedihin, Targeted Advances in Lithium-ion Batteries: A Critical Review of Synergetic Improvements in Energy Density, Life Cycle, and Safety, *American Journal of Quantum Chemistry and Molecular Spectroscopy* **9** (2025) 12-30. https://doi.org/10.11648/j.ajqcms.20250901.12

[2] J. Chattopadhyay, T. S. Pathak, D. M. F. Santos, Applications of Polymer Electrolytes in Lithium-Ion Batteries: A Review, *Polymers* **15** (2023) 3907. https://doi.org/10.3390/polym15193907.

[3] J. Liang, J. Luo, Q. Sun, X. Yang, R. Li, X. Sun, Recent progress on solid-state hybrid electrolytes for solid-state lithium batteries, *Energy Storage Materials* **21** (2019) 308-334. https://doi.org/10.1016/j.ensm.2019.06.021

[4] D. Ahmed, K. M. Maraz, Polymer electrolyte design strategies for high-performance and safe lithium-ion batteries: Recent developments and future prospects, *Materials Engineering Research* **5** (2023) 245-255. https://doi.org/10.25082/mer.2023.01.001

[5] N. Yazie, D. Worku, N. Gabbiye, A. Alemayehu, Z. Getahun, M. Dagnew, Development of polymer blend electrolytes for battery systems: recent progress, challenges, and future outlook, *Materials for Renewable and Sustainable Energy* **12** (2023) 73-94. https://doi.org/10.1007/s40243-023-00231-w

[6] [6] C. Cazan, Advances in Sustainable Polymeric Materials, *Polymers* **14** (2022) 4972. https://doi.org/10.3390/polym14224972
[7] J. Fu, Z. Li, X. Zhou, X. Guo, Ion transport in composite polymer electrolytes, *Materials Advances* **3** (2022) 3809-3819. https://doi.org/10.1039/D2MA00215A.
[8] D. Vanitha, S. A. Bahadur, N. Nallamuthu, S. Athimoolam, A. Manikandan, Electrical Impedance Studies on Sodium Ion Conducting Composite Blend Polymer Electrolyte, *Journal of Inorganic and Organometallic Polymers and Materials* **27** (2017) 257-265. https://doi.org/10.1007/s10904-016-0468-6
[9] S. S. Devangamath, B. Lobo, S. P. Masti, S. Narasagoudr, Thermal, mechanical, and AC electrical studies of PVA-PEG-$Ag_2S$ polymer hybrid material, *Journal of Materials Science: Materials in Electronics* **31** (2020) 2904-2917. https://doi.org/10.1007/s10854-019-02835-3
[10] Y. Mallaiah, V. R. Jeedi, R. Swarnalatha, A. Raju, S. Narender Reddy, A. Sadananda Chary, Impact of polymer blending on ionic conduction mechanism and dielectric properties of sodium based PEO-PVdF solid polymer electrolyte systems, *Journal of Physics and Chemistry of Solids* **155** (2021) 110096. https://doi.org/10.1016/j.jpcs.2021.110096
[11] H. T. Ahmed, O. G. Abdullah, Preparation and composition optimization of PEO:MC polymer blend films to enhance electrical conductivity, *Polymers* **11** (2019) 853. https://doi.org/10.3390/polym11050853
[12] S. A. S. Sharmizam, H. Hanibah, U. M. Tukur, N. Z. N. Hashim, A Review: Polymer Blend Electrolyte Systems as a Promising Alternative for Improving Ionic Conductivity, *Malaysian Journal of Chemistry* **26** (2024) 137-156. https://doi.org/10.55373/mjchem.v26i4.137
[13] S. Sowmiya, C. Shanthi, S. Selvasekarapandian, Development of sodium-ion conducting biopolymer electrolyte membrane based on Agar-Agar with sodium perchlorate ($NaClO_4$) using ethylene carbonate (EC) as a plasticizer for primary Na-ion battery, *Digest Journal of Nanomaterials and Biostructures* **18** (2023) 1537-1555. https://doi.org/10.15251/DJNB.2023.184.1537
[14] R. T. Abdulwahid, S. B. Aziz, M. F. Z. Kadir, Replacing synthetic polymer electrolytes in energy storage with flexible biodegradable alternatives: sustainable green biopolymer blend electrolyte for supercapacitor device, *Materials Today Sustainability* **23** (2023) 100472. https://doi.org/10.1016/j.mtsust.2023.100472
[15] P. Nayak, Y. N. Sudhakar, S. De, Ismayil, S. K. Shetty, Optimization of Chitosan:Methylcellulose polyblend to obtain highly amorphous polymer matrix useful for ion transportation, *Indian Journal of Physics* **97** (2023) 3483-3493. https://doi.org/10.1007/s12648-023-02684-1
[16] S. B. Aziz, M. H. Hamsan, M. F. Z. Kadir, W. O. Karim, R. M. Abdullah, Development of polymer blend electrolyte membranes based on chitosan:Dextran with high ion transport properties for EDLC application, *International Journal of Molecular Sciences* **20** (2019) 3369. https://doi.org/10.3390/ijms20133369
[17] L. Liang, Q. Cheng, Z. Yang, X. Lin, Y. Chen, X. Luo, Incorporation of phytic acid modified covalent organic polymers into gellan gum-chitosan gel network for selective adsorption of uranium: an experimental and DFT study, *Journal of Radioanalytical and Nuclear Chemistry* **334** (2025) 653-665. https://doi.org/10.1007/s10967-024-09812-z
[18] B. K. Kim, K. Park, Mass Transport Properties and Influence of Natural Convection for Voltammetry at the Agarose Hydrogel Interface, *Journal of Electrochemical Science and Technology* **13** (2022) 347-353. https://doi.org/10.33961/jecst.2022.00129
[19] P. Pandurangan, Recent Progression and Opportunities of Polysaccharide Assisted Bio-Electrolyte Membranes for Rechargeable Charge Storage and Conversion Devices, *Electrochem* **4** (2023) 212-238. https://doi.org/10.3390/electrochem4020015

[20] A. A. Shamsuri, R. Daik, Plasticizing effect of choline chloride/urea eutectic-based ionic liquid on physicochemical properties of agarose films, *BioResources* **7** (2012) 4760-4775. https://bioresources.cnr.ncsu.edu/resources/plasticizing-effect-of-choline-chlorideurea-eutectic-based-ionic-liquid-on-physicochemical-properties-of-agarose-films/
[21] S. Kumar, M. K. Singh, M. Z. A. Yahya, I. S. M. Noor, P. K. Singh, Structural, Electrochemical, and Dielectric Studies of Phytagel and 1-ethyl-3-methylimidazolium Tricyanomethanide-based Bio-polymer Electrolytes, *Zaštita materijala (Materials Protection)* **65** (2024) 703-711. https://doi.org/10.62638/ZasMat1050
[22] S. Aafrin Hazaana, A. Joseph, S. Selvasekarapandian, R. Meera Naachiyar, M. Vengadesh Krishna, N. Muniraj Vignesh, Development and characterization of biopolymer electrolyte based on gellan gum (GG) with lithium chloride (LiCl) for the application of electrochemical devices, *Polymer Bulletin* **80** (2023) 5291-5311. https://doi.org/10.1007/s00289-022-04316-w
[23] C. Naveen, M. Muthuvinayagam, K. A. Alrashidi, S. Mohammad, S. Vigneshwaran, S. V. Arunachalam, M. I. N. Isa, Investigations on electrical, electrochemical, and thermal properties of gelatine-based novel biopolymer electrolytes for energy storage applications, *Ionics* **30** (2024) 6097-6111. https://doi.org/10.1007/s11581-024-05750-8
[24] G. K. Abilova, S. F. Nasibullin, K. Ilyassov, A. N. Adilov, M. K. Akhmetova, R. I. Moustafine, Y. T. Muratov, S. E. Kudaibergenov, V. V. Khutoryanskiy, Mucoadhesive gellan gum/poly(2-ethyl-2-oxazoline) films for ocular delivery of pilocarpine hydrochloride, *Journal of Drug Delivery Science and Technology* **104** (2025) 106492. https://doi.org/10.1016/j.jddst.2024.106492
[25] X. C. Chen, R. L. Sacci, N. C. Osti, M. Tyagi, Y. Wang, J. K. Keum, N. J. Dudney, Study of the Segmental Dynamics and Ion Transport of Solid Polymer Electrolytes in the Semi-crystalline State, *Frontiers in Chemistry* **8** (2021) 592604. https://doi.org/10.3389/fchem.2020.592604
[26] D. H. Shin, S. J. Kim, Electrochemical Characteristics with NaCl Concentrations on Stainless Steels of Metallic Bipolar Plates for PEMFCs, *Coatings* **13** (2023) 109. https://doi.org/10.3390/coatings13010109
[27] R. Holze, Overoxidation of Intrinsically Conducting Polymers, *Polymers* **14** (2022) 1584. https://doi.org/10.3390/polym14081584
[28] I. Rendón-Enríquez, A. Palma-Cando, F. Körber, F. Niebisch, M. Forster, M. W. Tausch, U. Scherf, Thin Polymer Films by Oxidative or Reductive Electropolymerization and Their Application in Electrochromic Windows and Thin-Film Sensors, *Molecules* **28** (2023) 883. https://doi.org/10.3390/molecules28020883
[29] I. L. Johansson, C. Sangeland, T. Uemiya, F. Iwasaki, M. Yoshizawa-Fujita, D. Brandell, J. Mindemark, Improving the Electrochemical Stability of a Polyester-Polycarbonate Solid Polymer Electrolyte by Zwitterionic Additives, *ACS Applied Energy Materials* **5** (2022) 10002-10012. https://doi.org/10.1021/acsaem.2c01641
[30] A. Méry, S. Rousselot, D. Lepage, M. Dollé, A critical review for an accurate electrochemical stability window measurement of solid polymer and composite electrolytes, *Materials* **14** (2021) 3840. https://doi.org/10.3390/ma14143840
[31] M. Basappa, H. Ganesha, S. Veeresh, Y. S. Nagaraju, M. Vandana, H. Vijeth, H. Devendrappa, Preparation, characterization, and electrochemical properties of PEO/PVDF blend films, *Chemical Physics Letters* **799** (2022) 139609. https://doi.org/10.1016/j.cplett.2022.139609
[32] M. Airoldi, U. Steiner, I. Gunkel, The Role of Interfacial Effects in the Impedance of Nanostructured Solid Polymer Electrolytes, *Batteries* **10** (2024) 401. https://doi.org/10.3390/batteries10110401
[33] J. P. Coote, S. K. J. Adotey, J. R. Sangoro, G. E. Stein, Interfacial Effects in Conductivity Measurements of Block Copolymer Electrolytes, *ACS Polymers Au* **3** (2023) 331-343. https://doi.org/10.1021/acspolymersau.2c00068

[34] D. Sharon, P. Bennington, C. Liu, Y. Kambe, B. X. Dong, V. F. Burnett, M. Dolejsi, G. Grocke, S. N. Patel, P. F. Nealey, Interrogation of Electrochemical Properties of Polymer Electrolyte Thin Films with Interdigitated Electrodes, *Journal of The Electrochemical Society* **165** (2018) H1028-H1039. https://doi.org/10.1149/2.0291816jes

[35] D. Zhang, X. Meng, W. Hou, W. Hu, J. Mo, T. Yang, W. Zhang, Q. Fan, L. Liu, B. Jiang, L. Chu, M. Li, Solid polymer electrolytes: Ion conduction mechanisms and enhancement strategies, *Nano Research Energy* **2** (2023) 9120050. https://doi.org/10.26599/NRE.2023.9120050

[36] R. A. K. Abdl Aali, S. T. G. Al-Sahlany, Gellan Gum as a Unique Microbial Polysaccharide: Its Characteristics, Synthesis, and Current Application Trends, *Gels* **10** (2024) 183. https://doi.org/10.3390/gels10030183

[37] B. K. Wheatle, N. A. Lynd, V. Ganesan, Effect of Polymer Polarity on Ion Transport: A Competition between Ion Aggregation and Polymer Segmental Dynamics, *ACS Macro Letters* **7** (2018) 1149-1154. https://doi.org/10.1021/acsmacrolett.8b00594

[38] M. H. Razali, N. A. Ismail, U. M. Osman, K. A. M. Amin, Mechanical and Physical Properties of Gellan Gum (GG) Biofilm: Effect of Glycerol, *ASM Science Journal* Special Issue **2018(1) AiMS2018** (2018) 158-165. https://www.akademisains.gov.my/asmsj/article/mechanical-and-physical-properties-of-gellan-gum-gg-biofilm-effect-of-glycerol/

[39] M. Kani Ajay Babu, S. S. Jayabalakrishnan, S. Selvasekarapandian, S. Aafrin Hazaana, R. Meera Naachiyar, N. Muniraj Vignesh, Development and characterization of biopolymer electrolyte based on gellan gum for the fabrication of solid-state sodium-ion battery, *Ionics* **29** (2023) 5249-5265. https://doi.org/10.1007/s11581-023-05210-9

[40] N. S. M. Rafi, S. Z. Z. Abidin, S. R. Majid, R. Zakaria, Preparation of Agarose-based Biopolymer Electrolytes Containing Calcium Thiocyanate: Electrical and Electrochemical Properties, *International Journal of Electrochemical Science* **17** (2022) 220713. https://doi.org/10.20964/2022.07.21

[41] R. Pradeep, V. Siva, M. A. Jothi, A. Murugan, A. Shameem, S. Sanjana, E. Hemnath, A. G. Al-Sehemi, Structural, surface morphological and dielectric studies of guanidinium salt incorporated poly(ethylene oxide)/poly(vinyl pyrrolidone) solid polymer electrolytes, *Heliyon* **10** (2024) e23524. https://doi.org/10.1016/j.heliyon.2023.e23524

[42] N. I. Ali, S. N. Zaharuddin, N. A. S. M. Azis, N. S. M. Rafi, S. Z. Z. Abidin, Conductivity and morphological studies of poly(vinyl alcohol)-magnesium triflate-ethylene carbonate gel polymer electrolyte, *Scientific Research Journal* **18** (2021) 161-175. https://doi.org/10.24191/srj.v18i2.13041

[43] N. F. Sulthan Hussain, S. Z. Zainal Abidin, M. K. Yaakob, S. R. Che Balian, Elucidating the electronic structure, ionic transport and electrochemical characterization of agarose-based biopolymer electrolytes modulated by $NaNO_3$ and $NaPF_6$: A combined density functional theory and experimental study, *Solid State Ionics* **443** (2026) 117250. https://doi.org/10.1016/j.ssi.2026.117250

[44] M. M. Nasef, E. A. El-Hefian, S. Saalah, A. H. Yahaya, Preparation and properties of non-crosslinked and ionically crosslinked chitosan/agar blended hydrogel films, *E-Journal of Chemistry* **8** (2011) S409-S419. https://doi.org/10.1155/2011/513204

[45] A. Astanina, J. T. Koivisto, M. Hannula, T. Salminen, M. Kellomäki, J. Massera, Chemical interactions in composites of gellan gum and bioactive glass: self-crosslinking and in vitro dissolution, *Frontiers in Chemistry* **11** (2023) 1133374. https://doi.org/10.3389/fchem.2023.1133374

[46] M. Baublytė, J. Kupčiūnaitė, M. Liubinienė, A. Beganskienė, Hydrogels—a desirable alternative to water paper restoring procedures: impacting paper properties, *Chemija* **33** (2022) 136-147. https://doi.org/10.6001/chemija.v33i4.4807

[47] N. I. Ali, S. Z. Z. Abidin, S. R. Majid, The High-Performance Polymer Electrolytes Based on Agarose-Mg($ClO_4$)$_2$ for Application in Electrochemical Energy Storage Devices, *Journal of Advanced Research in Fluid Mechanics and Thermal Sciences* **118** (2024) 65-85. https://doi.org/10.37934/arfmts.118.1.6585

[48] K. H. Arifin, Z. Osman, N. Tamchek, M. I. M. Ghazali, I. M. Noor, Impact of ionic liquid on structural, thermal and transport properties in gellan gum-lithium triflate solid polymer electrolyte, *Synthetic Metals* **297** (2023) 117406. https://doi.org/10.1016/j.synthmet.2023.117406